Relativistic chaos in the driven harmonic oscillator

Jung-Hoon Kim and Hai-Woong Lee
Department of Physics, Korea Advanced Institute of Science and Technology, Taejon, 305-701, Korea
(Received 20 May 1994)

The classical motion of the relativistic harmonic oscillator driven by a sinusoidal force exhibits resonance overlap and chaos normally associated with driven nonlinear oscillators.

PACS number(s): 05.45.+b

The driven harmonic oscillator in the nonrelativistic regime is, of course, the standard textbook model for a linear system subject to external perturbation. Its relativistic counterpart, on the other hand, contains nonlinear terms in the equation of motion and can exhibit features such as resonance overlap and chaos [1,2] that are normally attributed to driven nonlinear systems.

The Hamiltonian for the relativistic one-dimensional harmonic oscillator of mass m and force constant k driven by a sinusoidal force of amplitude F_0 and frequency ω is given by [3]

$$H = \sqrt{p^2c^2 + m^2c^4} + \frac{1}{2}kq^2 + qF_0 \cos\omega t \ , \tag{1}$$

which leads immediately to Hamilton's equations,

$$\frac{dq}{dt} = \frac{pc^2}{\sqrt{p^2c^2 + m^2c^4}}, \tag{2}$$

$$\frac{dp}{dt} = -kq - F_0 \cos\omega t. \tag{3}$$

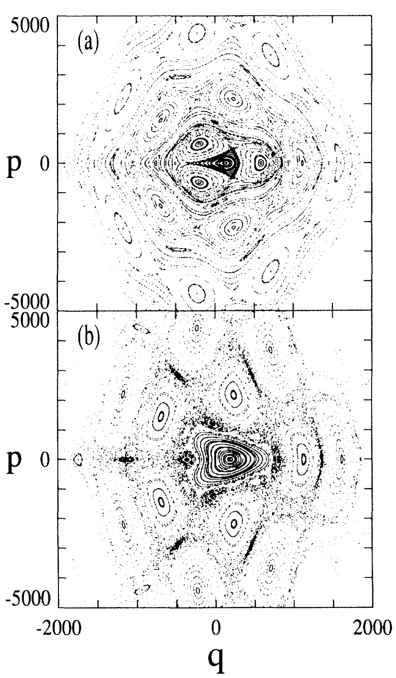

FIG. 1. Poincaré phase-space map for the driven relativistic harmonic oscillator with m (mass)=1, k (force constant)=1, ω (driving frequency)=2 in a unit system in which c (speed of light)=300. The amplitude of the driving force is 500 for (a) and 1500 for (b).

The Poincaré phase-space map obtained by numerically integrating Eqs. (2) and (3) for a series of different initial conditions is shown in Fig. 1(a) [Fig. 1(b)], where the parameter values are chosen to be $m = 1, k = 1, \omega = 2, F_0 = 500$ [$F_0 = 1500$] in a unit system in which $c = 300$. Resonances of odd periods induced by the driving force are clearly seen. We note that no even resonances are formed (in the first order) due to the symmetry of the potential. At $F_0 = 500$, each period-n resonance is clearly separated from neighboring resonances. At $F_0 = 1500$, however, the overlap between neighboring resonances has occurred in the separatrix regions; in particular, we observe that the period-3 resonance has been completely destroyed and the chaotic sea occupies a large portion of the phase space. The nature of the regular and chaotic motions that coexist at $F_0 = 1500$ is contrasted in Fig. 2, where the time development of the oscillator energy $\mathcal{E}(\mathcal{E} = \sqrt{p^2c^2 + m^2c^4} + \frac{1}{2}kq^2)$ is plotted for the motion started at one of the elliptic fixed points of the period-5 and period-7 resonances and for the motion started at a point in the chaotic region near the period-5

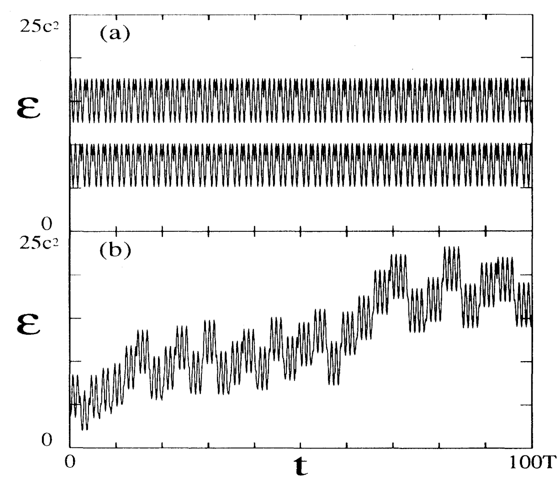

FIG. 2. The oscillator energy $\mathcal{E} = \sqrt{p^2c^2 + m^2c^4} + \frac{1}{2}kq^2$ vs time at $F_0 = 1500$. The top and bottom curves in (a) show the time development of $\mathcal{E}$ when the motion is started at the elliptic fixed points ($q = 1614$, $p = 0$) and ($q = 1128$, $p = 0$) of the period-7 and period-5 resonances, respectively, and (b) plots $\mathcal{E}$ for the case when the motion is started at the phase-space point ($q = -683$, $p = 156$) located in the chaotic region.

resonance.

The oscillator energy $\mathcal{E}_n$ at which the period-n resonance is formed can conveniently be estimated by means of the technique based on action-angle variables often used to analyze resonances induced in driven nonlinear systems [1,2,4]. In order to find $\mathcal{E}_n$ in the limit $F_0 \to 0$, we first consider our relativistic oscillator in the absence of the driving force. The action variable I ($I = \frac{1}{2\pi}\oint p dq$) can be shown to be given by

$$I = \frac{4a}{3\pi c}\left[\mathcal{E}E\left(\frac{b}{a}\right) - mc^2 K\left(\frac{b}{a}\right)\right], \tag{4}$$

where E and K, respectively, are the complete elliptic integrals of the second and first kinds, $a = \sqrt{\frac{2}{k}(\mathcal{E}+mc^2)}$, and b is the amplitude of oscillation given by $b = \sqrt{\frac{2}{k}(\mathcal{E}-mc^2)}$. With application of an external force of frequency ω, the period-n resonance occurs in the limit $F_0 \to 0$ at $I = I_n$ that satisfies $n\Omega(I_n) = \omega$, where $\Omega = \frac{\partial \mathcal{E}(I)}{\partial I}$. The energy $\mathcal{E}_n$ can thus be determined by finding the root of the equation $n = \omega\frac{\partial I(\mathcal{E})}{\partial \mathcal{E}}$. Using again the parameter values, $m = 1, k = 1, \omega = 2$ and $c = 300$ and evaluating the complete elliptic integrals by expanding them in series of $\frac{b}{a}$, we can compute $\frac{\partial I(\mathcal{E})}{\partial \mathcal{E}}$ as a function of $\mathcal{E}$. Results of our computation, shown in Fig. 3, allow an immediate evaluation of $\mathcal{E}_n$. For example, the period-5 (period-7) resonance occurs at $\mathcal{E}_5 \cong 7.6c^2$ ($\mathcal{E}_7 \cong 15c^2$), from which we can estimate the position of one of the elliptic fixed points of the resonance to be $q \cong 1090$, $p \cong 0$ ($q \cong 1590, p \cong 0$). If the motion is started at this fixed point, the momentum at $q = 0$ reaches the value of ~ 2270 (~ 4510), which corresponds to the velocity of $v \cong 297.4 \cong 0.991c$ ($v \cong 299.3 \cong 0.998c$). We mention that the above estimate of the position of the elliptic fixed point(in the limit $F_0 \to 0$) is in good agreement with our computer simulation, which yielded $q \cong 1110$, $p \cong 0$ ($q \cong 1600$, $p \cong 0$) at $F_0 = 500$.

Some insight into the motion being considered can be obtained by rewriting Eqs. (2) and (3) as

$$\frac{dq}{dt} = v, \tag{5}$$

$$\frac{dv}{dt} = -\frac{k'}{m}q - \frac{F_0'}{m}\cos\omega t, \tag{6}$$

where $k' = k/\gamma^3, F_0' = F_0/\gamma^3$ and $\gamma = 1/\sqrt{1-\frac{v^2}{c^2}}$. Thus, the motion of the driven relativistic harmonic oscillator is equivalent to that of a nonrelativistic harmonic oscillator with a velocity dependent force constant driven by a velocity dependent force. It should be noted, in particular, that both k' and F_0' approach zero as v approaches c. Thus, the oscillator at high energies behaves much like a free particle except near the turning points. The Poincaré map shown in Fig. 4 with q and v as parameters suggests some similarity between the relativistic oscillator at high energies and the nonrelativistic particle in an infinite square-well potential [4,5]. The main difference, however, is that, while the amplitude of the motion is fixed for the square-well system, it is rather a fast increasing function of energy $\mathcal{E}$ for the relativistic oscillator. As a consequence, a higher-period resonance is located at a higher energy for the case of the relativistic oscillator in opposition to the situation in the square-well system.

An alternative view of the motion of the driven relativistic oscillator can be provided by making use of the canonical transformation [3] with a generating function $F(q,Q) = qQ$ which yields $Q = p, P = -q$. Upon substitution of $P' = P - \frac{F_0}{k}\cos\omega t$, Hamilton's equations in the transformed coordinates take the form

$$\frac{dQ}{dt} = kP', \tag{7}$$

$$\frac{dP'}{dt} = -\frac{Qc^2}{\sqrt{Q^2c^2+m^2c^4}} + \frac{\omega}{k}F_0\sin\omega t. \tag{8}$$

The driven relativistic oscillator is thus transformed to a driven nonrelativistic nonlinear oscillator with the potential $V(Q) = \sqrt{Q^2c^2+m^2c^4}$.

It is worth noting that the nonlinearity arising from the term $\sqrt{p^2c^2+m^2c^4}$ in the Hamiltonian, which is, of course, responsible for the chaotic behavior we observed, does not always guarantee chaos. In order to show this, let us consider a relativistic particle in a linear potential $V(q) = Aq + B$ (A and B are constants) driven by a

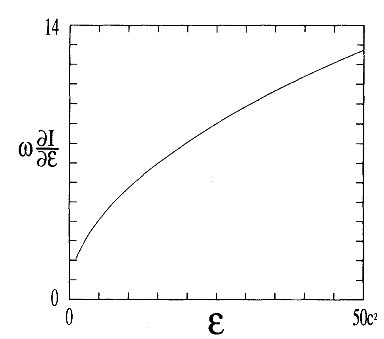

FIG. 3. $\omega\frac{\partial I}{\partial \mathcal{E}}$ vs $\mathcal{E}$. The energy $\mathcal{E}_n$ at which the period-n resonance is formed can be identified as the value of $\mathcal{E}$ on the horizontal axis corresponding to the value n on the vertical axis.

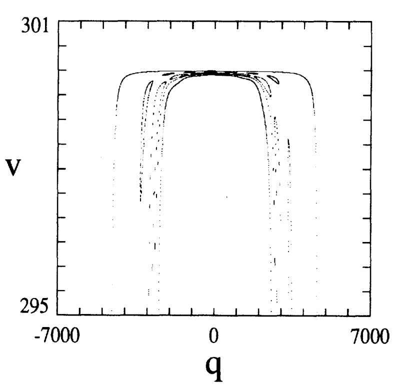

FIG. 4. Poincaré map in (q,v) space for the same system as in Fig. 1(a) obtained with five different initial points (0, 299.99), (0, 299.97), (0, 299.95), (0, 299.93) and (0, 299.91).

sinusoidal force. Hamilton's equations now read

$$\frac{dq}{dt} = \frac{pc^2}{\sqrt{p^2c^2 + m^2c^4}}, \tag{9}$$

$$\frac{dp}{dt} = -A - F_0 \cos \omega t, \tag{10}$$

which are integrable. Relativistic chaos requires at least a quadratic potential, while nonrelativistic chaos needs at least a cubic term in the potential.

Finally, we mention that chaotic dynamics of relativistic particles has been considered in the past. It has been shown that chaos can be exhibited by, for example, relativistic electrons propagating through a spatially inhomogeneous wiggler field in a free electron laser system [6], relativistic electrons in the electric field of an electrostatic wave packet [7], relativistic electrons in a free electron laser system with gain modulation [8], the driven relativistic electron plasma wave [9], and the driven relativistic Duffing oscillator [10]. Chaos observed in the present work, however, seems more fundamental in that it arises from nonlinearity always present in the relativistic Hamiltonian.

ACKNOWLEDGMENTS

This research was supported in part by a KAIST research grant and by the Ministry of Science and Technology of Korea.

[1] B. V. Chirikov, Phys. Rep. **52**, 263 (1979).
[2] D. F. Escande and F. Doveil, J. Stat. Phys. **26**, 257 (1981).
[3] H. Goldstein, *Classical Mechanics*, 2nd ed. (Addison-Wesley, Reading, 1980).
[4] W. A. Lin and L. E. Reichl, Physica D **19**, 145 (1986).
[5] J. Y. Shin and H. W. Lee, J. Kor. Phys. Soc. **27**, 5 (1994).
[6] C. Chen and R. C. Davidson, Phys. Rev. A **42**, 5041 (1990).
[7] A. A. Chernikov, T. Tel, G. Vattay, and G. M. Zaslavsky, Phys. Rev. A **40**, 4072 (1989).
[8] M. Billardon, Phys. Rev. Lett. **65**, 713 (1990).
[9] W. P. Leemans, C. Joshi, W. B. Mori, C. E. Clayton, and T. W. Johnston, Phys. Rev. A **46**, 5112 (1992).
[10] W. C. Schieve and L. P. Horwitz, Phys. Lett. A **156**, 140 (1991).